

Methods

S1 Extraction and determination of chlorophyll pigments

Three replicates of approximately 0.2 grams of dry leaf tissue per bryophyte species were gathered and kept at 4°C. Later, they were ground in 95% ethanol with quartz sand and CaCO₃ powder (about 0.5g each) using a mortar and pestle that had been cooled to 4°C. This was done in dim light to prevent degradation of chlorophyll pigments. The spectrophotometer was used to measure the absorbance of extracted chlorophyll pigments at 649 nm and 665 nm. The concentrations of chlorophyll a (Chl a), chlorophyll b (Chl b), and total chlorophyll (Chl) were then calculated as following formulas.

$$\text{Chla (mg g}^{-1}\text{)} = 13.95A_{664} - 6.88A_{649}$$

$$\text{Chb (mg g}^{-1}\text{)} = 24.96A_{649} - 7.32A_{655}$$

$$\text{Chl (mg g}^{-1}\text{)} = \text{Chla} + \text{Chlb}$$

S2 Response of photosynthetic rate to light

We collected five replicate samples of shoot material from each species from August to October 2021, for which photosynthetic light response curves were measured using a portable photosynthesis system (GFS-3000, Walz, Effeltrich, Germany). After dirty and dead tissue had been removed, 2.5-4.5 cm long samples of stem material were cut from the apex or whole plant by removing the rhizoids; the stem material was then submerged and saturated in distilled water for 1 h. Excessive superficially adherent water was then carefully removed using a paper towel before samples were placed in a whole plant chamber attached to a portable infrared gas analyzer to determine net photosynthetic rates; a full spectrum light source that was placed on top of the chamber provided cold illumination to avoid dramatic changes in temperature. Photosynthetic rate based on bryophyte area and mass is lower than in vascular plants; therefore, we set the flow rate at 400 $\mu\text{mol m}^{-2} \text{s}^{-2}$ in ambient conditions (25°C; 80%RH). Light response curves were determined using 13 photosynthetically active radiation (PAR) gradients (0, 25, 50, 100, 150, 200, 250, 300, 400, 500, 600, 800, 1000 $\mu\text{mol m}^{-2} \text{s}^{-1}$). Light response curves were fitted to a modified rectangular hyperbola. Samples were oven-dried for 48 h at 70°C after trait measurement to determine dry mass.

S3 Chlorophyll fluorescence

Chlorophyll fluorescence signals were measured using a PAM fluorometer (PAM-250, Walz, Effeltrich, Germany) from five replicate leaf samples per species. Before measurement, the leaf samples were dark-adapted for 20 minutes and then saturated in distilled water. Two or three overlapping leaves were selected on shoots to fill the measuring area (with a diameter of 0.5 cm). The initial minimal fluorescence efficiency in the dark-adapted state (F_0) was assessed by exposing the leaf material to a weak, modulated beam. A saturation pulse of approximately $5500 \mu\text{mol m}^{-2} \text{s}^{-1}$ for 0.7 seconds was then applied to assess maximal photochemical efficiency when PSII reaction centers were closed (F_m). Minimal and maximal Chl fluorescence efficiency and the steady-state Chl fluorescence efficiency in the light-adapted state (F_0' , F_m' and F_s) were measured using actinic illumination (approximately $110 \mu\text{mol m}^{-2} \text{s}^{-1}$) and saturating illumination, respectively. The maximal photochemical efficiency of PSII in the dark-adapted state (F_v/F_m), where F_v is variable fluorescence yield, was calculated as $F_v = F_m - F_0$. The actual photochemical efficiency of PSII in the light-adapted state (ϕPSII) was calculated as $\phi\text{PSII} = (F_m' - F_s)/F_m'$. Photochemical quenching (qP) was calculated as $qP = (F_m' - F_s)/(F_m' - F_0')$, and nonphotochemical quenching (NPQ) was derived from $\text{NPQ} = (F_m - F_m')/F_m'$.

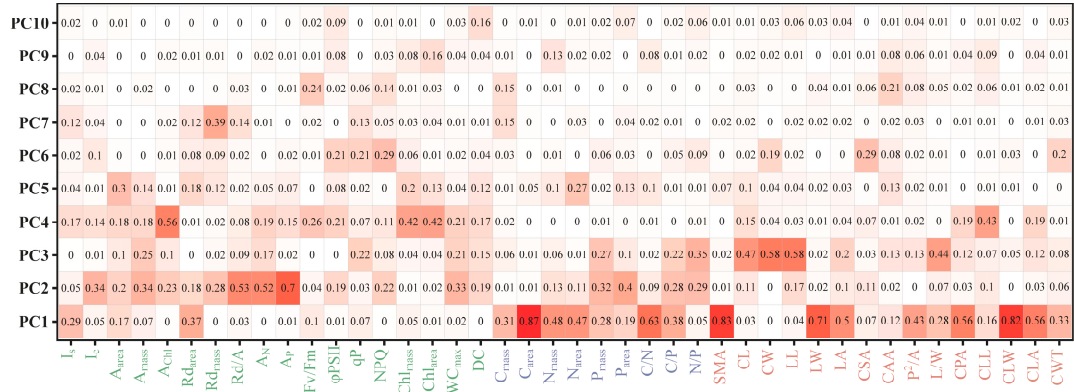
Table S1 Function traits data of the 11 species of mosses in the study. CBL: Chebaling, GS: Guanshan. The details are seen in Table S1.csv.

Table S2 Sampling time and the location of the patches in Chebaling National Nature Reserve (CBL) and Guanshan National Nature Reserve (GS). The details are seen in Table S2.csv.

Table S3. Results of likelihood-ratio tests for the sample scores of the first four PCA axes, testing whether sample scores of the first four PCA axes by comparing the full model (i.e., region/species as a random effect) with a nested subset (i.e., specie as with a random effect). A significant difference between the two models indicates that regions affect the scores of species in PC2.

	AIC	BIC	logLik	Deviance	Chisq	P
PC1						
Species	179.19	185.16	-86.596	173.19		
Region/Species	199.29	207.24	-95.643	191.29	0	1
PC2						
Species	252.31	258.27	-123.15	246.31		
Region/Species	248.30	256.26	-120.15	240.30	6.003	0.014*
PC3						
Species	194.57	200.53	-94.284	188.57		
Region/Species	207.15	215.11	-99.577	199.15	0	1
PC4						
Species	205.90	211.87	-99.952	199.90		
Region/Species	213.23	221.18	-102.614	205.23	0	1

A



B

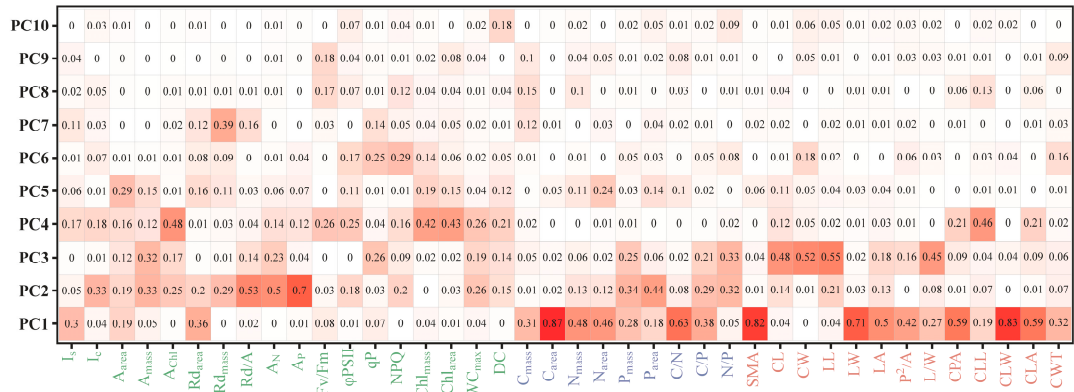


Figure S1 The variance distribution of the function traits (A: 42 traits; B: 40 traits) projected on the first ten PCA axes.

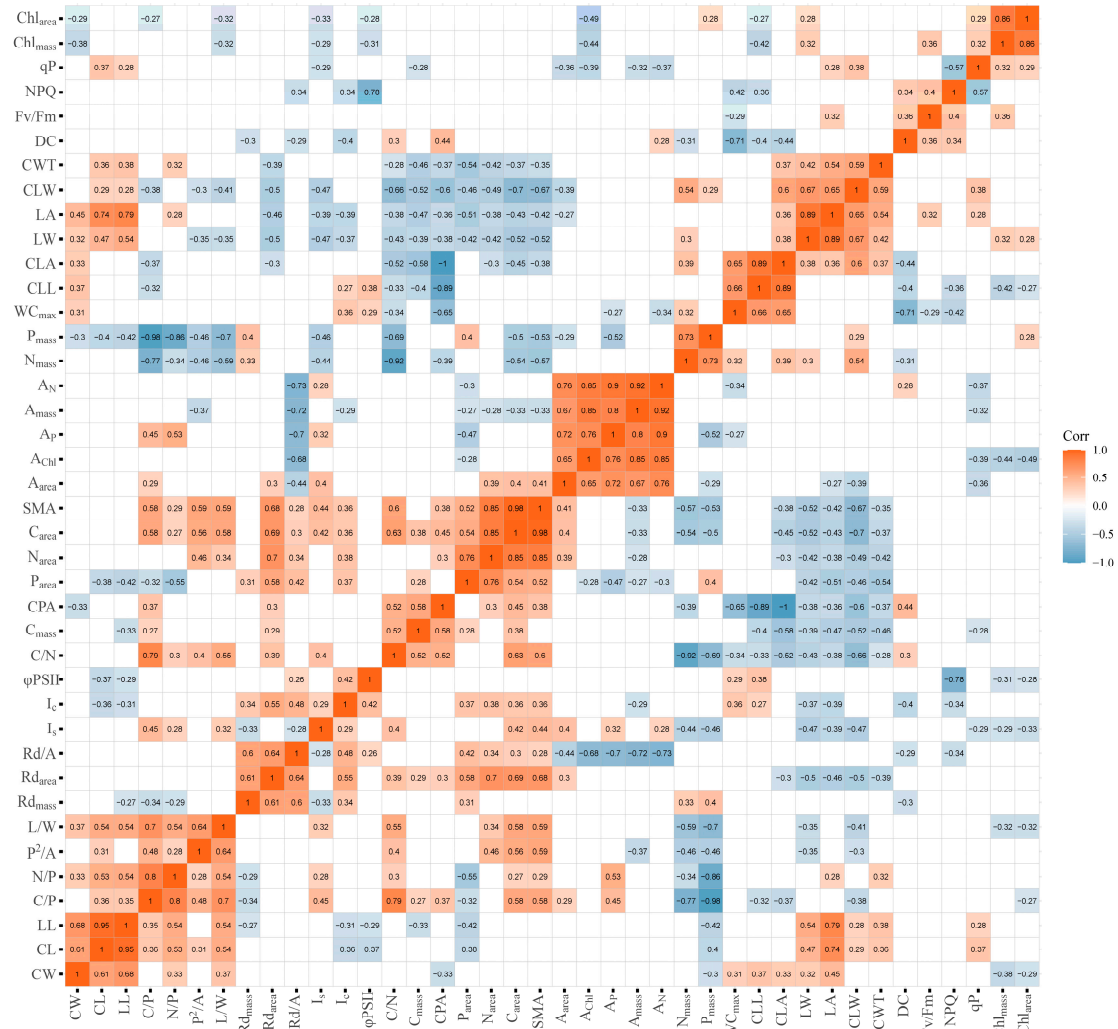


Figure S2 Bi-variate relationship between function traits evaluated by Spearman correlation. Only the significant relationship (p<0.05) was shown in the heatmap.

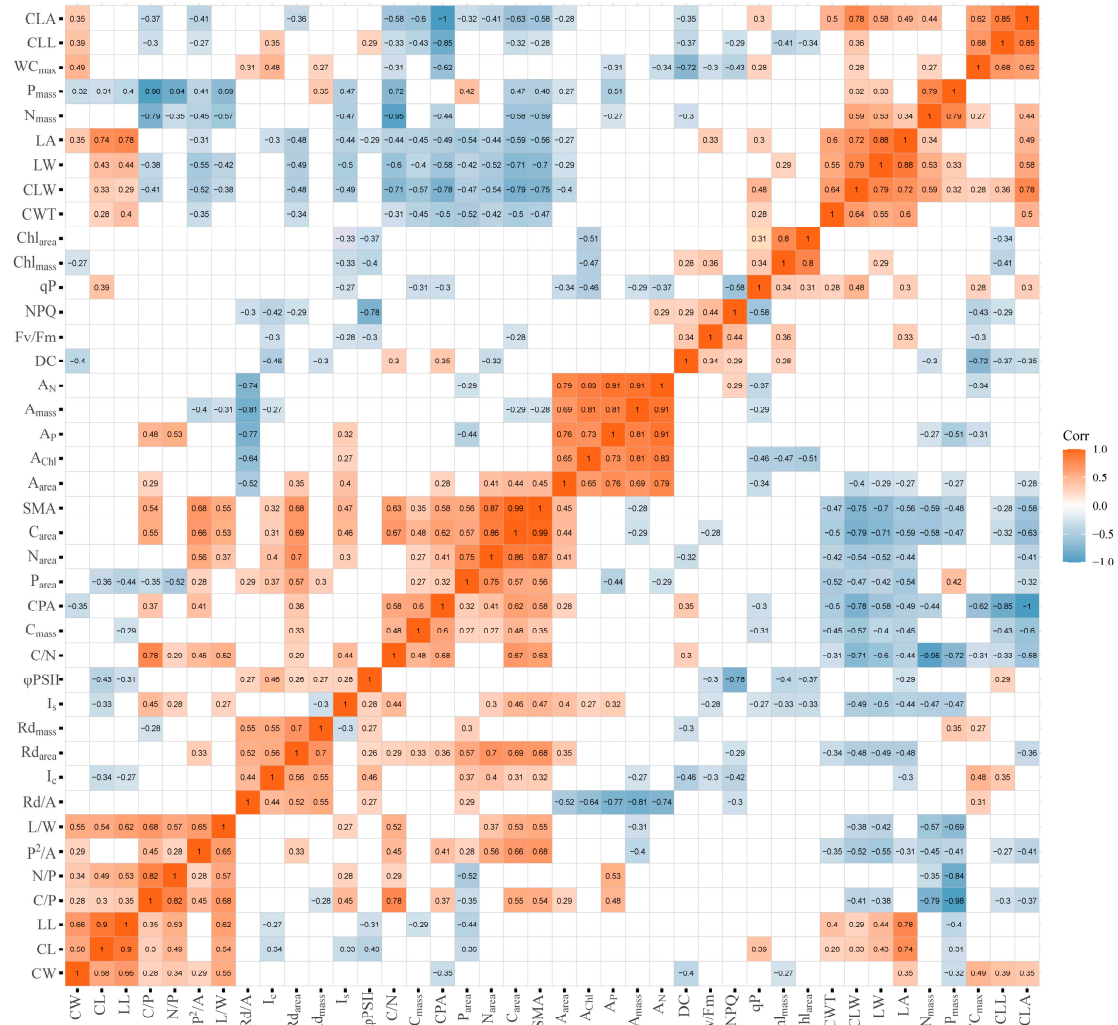


Figure S3 Bi-variate relationship between function traits evaluated by Pearson correlation. Only the significant relationship ($p < 0.05$) was shown in the heatmap.